



Mitochondria and NMDA Receptor-Dependent Toxicity of Berberine Sensitizes Neurons to Glutamate and Rotenone Injury

Kai Kysenius, Cecilia A. Brunello, Henri J. Huttunen*

Neuroscience Center, University of Helsinki, Helsinki, Finland

Abstract

The global incidence of metabolic and age-related diseases, including type 2 diabetes and Alzheimer's disease, is on the rise. In addition to traditional pharmacotherapy, drug candidates from complementary and alternative medicine are actively being pursued for further drug development. Berberine, a nutraceutical traditionally used as an antibiotic, has recently been proposed to act as a multi-target protective agent against type 2 diabetes, dyslipidemias, ischemic brain injury and neurodegenerative diseases, such as Parkinson's and Alzheimer's disease. However, the safety profile of berberine remains controversial, as isolated reports suggest risks with acute toxicity, bradycardia and exacerbation of neurodegeneration. We report that low micromolar berberine causes rapid mitochondria-dependent toxicity in primary neurons characterized by mitochondrial swelling, increased oxidative stress, decreased mitochondrial membrane potential and depletion of ATP content. Berberine does not induce caspase-3 activation and the resulting neurotoxicity remains unaffected by pan-caspase inhibitor treatment. Interestingly, inhibition of NMDA receptors by memantine and MK-801 completely blocked berberine-induced neurotoxicity. Additionally, subtoxic nanomolar concentrations of berberine were sufficient to sensitize neurons to glutamate excitotoxicity and rotenone injury. Our study highlights the need for further safety assessment of berberine, especially due to its tendency to accumulate in the CNS and the risk of potential neurotoxicity as a consequence of increasing bioavailability of berberine.

Citation: Kysenius K, Brunello CA, Huttunen HJ (2014) Mitochondria and NMDA Receptor-Dependent Toxicity of Berberine Sensitizes Neurons to Glutamate and Rotenone Injury. PLoS ONE 9(9): e107129. doi:10.1371/journal.pone.0107129

Editor: Shao-Jun Tang, University of Texas Medical Branch, United States of America

Received: March 31, 2014; **Accepted:** August 14, 2014; **Published:** September 5, 2014

Copyright: © 2014 Kysenius et al. This is an open-access article distributed under the terms of the Creative Commons Attribution License, which permits unrestricted use, distribution, and reproduction in any medium, provided the original author and source are credited.

Data Availability: The authors confirm that all data underlying the findings are fully available without restriction. All relevant data are within the paper.

Funding: Research was funded by grants from the Academy of Finland (HJH) (grant numbers 218081 and 263762), the FGSN/Brain & Mind (KK) and GPBM/Integrative Life Science (CAB) doctoral programs and the University of Helsinki (KK, CAB, HJH). The funders had no role in study design, data collection and analysis, decision to publish, or preparation of the manuscript.

Competing Interests: Henri J. Huttunen is a part-time employee and shareholder of Herantis Pharma plc., which is unrelated to this study. There are no patents, products in development or marketed products to declare. This does not alter the authors' adherence to all the PLOS ONE policies on sharing data and materials.

* Email: Henri.Huttunen@helsinki.fi

Introduction

The number of patients with diabetes has more than doubled in three decades, and is currently estimated to be nearly 350 million [1]. Management of hyperglycemia is a key intervention strategy in diabetes. In addition to lifestyle-directed interventions, a variety of oral pharmacological agents that improve insulin sensitivity are used to treat type 2 diabetes (T2D) and the prediabetic state [2]. Similarly to diabetes, the prevalence of age-related neurodegenerative diseases, such as Alzheimer's disease (AD), is on the rise, affecting more than 34 million people worldwide [3]. For AD, only symptomatic pharmacotherapies are available. In addition to the industrial drug development efforts for T2D, AD and their prodromal phases, complementary and alternative medicine treatments are actively being explored.

The multifunctional natural compound berberine (BBR), a nutraceutical used in traditional Chinese and native American medicine for centuries, is the principal active component of barberry, goldenseal and other root extracts [4]. Recently, the pharmacological and bioactive properties of BBR have been extensively studied in a variety of models, both *in vitro* and *in vivo*, testing its potency against numerous indications, including

dyslipidemias [5], ischemia [6], diabetes [5], arrhythmias [7], cancer [8], Parkinson's disease, and Alzheimer's disease [9,10]. The proposed actions of BBR in metabolic disorders include insulin receptor upregulation, mitochondrial complex I inhibition, AMP-activated protein kinase (AMPK) activation, low-density lipoprotein (LDL) receptor upregulation, and proprotein convertase subtilisin kexin 9 (PCSK9) downregulation ([11], reviewed in [12]). Additionally, cholinesterase inhibition, monoamine oxidase inhibition, BACE1 inhibition and antioxidant activity comprise the proposed anti-AD effects of BBR [13–15]. Although numerous mechanisms have been proposed, the pharmacological actions of BBR remain incompletely understood, especially in the central nervous system (CNS).

The lack of clarity within BBR literature is partially due to the variability in the concentrations and formulations of BBR applied in both cell- and animal model-based studies. The common dosage range spans from 0.1 nM to 300 μ M, and from 5 mg to 100 mg/kg/day in *in vitro* and *in vivo* studies, respectively [13,16–19]. Pharmacological data suggest that berberine has poor bioavailability and that only nanomolar plasma concentrations are reached in both humans and animals [20]. According to several reports, however, BBR accumulates in organs such as

lungs, liver and the brain, resulting in effective concentrations in the low micromolar range [13,20–22]. Additionally, pro-drug development efforts aim at increasing BBR bioavailability [11,23]. BBR is generally considered safe for use in humans, but several reports have raised concerns over BBR toxicity and side effects, especially with increasing BBR concentrations [19,21,24–26].

The proposed anti- and pro-apoptotic roles of BBR are largely dose-dependent. In general, nanomolar BBR is believed to protect neuronal cells from ischemic insults, whereas cancer cell growth and proliferation is inhibited by high micromolar BBR [8,16]. Similarly, in the TgCRND8 mouse model of AD, a higher dosage (100 mg/kg/d versus 25 mg/kg/d) blunted the protective effects of BBR against amyloid plaque pathology and gliosis [13]. The mechanistic basis for the biphasic effects of BBR on neuronal viability remains incompletely characterized [27]. The proposed targets of BBR associated with neuronal viability include modulation of mitochondrial and caspase pathways, N-methyl-D-aspartate (NMDA) receptors, inhibition of potassium currents, and transcriptional regulation of lipoprotein receptors [20].

The characterization of BBR effects on neuronal viability remains incomplete. In this study, we assessed the effect of BBR on neuronal viability using cultured primary neurons: cerebellar granule neurons (CGN) and rat hippocampal neurons (HCN). We found that concentrations exceeding 1 μ M reduced neuronal viability in a caspase-independent manner characterized by early alterations of mitochondrial function and morphology. Cyclosporine A (CsA), a mitochondrial permeability transition pore (PTP) inhibitor, could partially prevent BBR toxicity independently of its calcineurin inhibitor activity. However, NMDA receptor antagonists MK-801 and memantine completely blocked this acute toxicity, indicating a central role for NMDA receptors in BBR-mediated cell death. Additionally, subtoxic nanomolar BBR pretreatment sensitized neurons to both glutamate excitotoxicity and rotenone-induced cell death. Our study provides mechanistic evidence of a neurotoxic mechanism of BBR that involves the NMDA receptors and mitochondria, predisposing neurons to glutamate excitotoxicity and mitochondria-targeting toxins.

Materials and Methods

Ethics statement

Animals were obtained from the Laboratory Animal Center, University of Helsinki. Animals were housed in controlled conditions (temperature +22°C, light from 08:00 to 18:00; humidity 50–60%), with fresh food and water available *ad libitum*. Tissue extraction from NMRI mice and Wistar rats was performed in accordance with the national and institutional guidelines approved by the University of Helsinki Laboratory Animal Center (permission number KEK11-019; approved 31.5.2011). Animals were euthanized by approved methods (CO₂ chamber and cervical dislocation) prior to the extraction of brain tissue used for primary neuronal culture preparation. A total of 65 P6–8 NMRI mouse pups and 4 Wistar pregnant rats and their litters were sacrificed for the generation of the primary cell cultures used to generate the data presented in this study.

Reagents

Berberine chloride, z-VAD-FMK, cyclosporine A, memantine, MK-801, and resazurin sodium salt were purchased from Sigma. FK506 (cat. no. Asc-223) was purchased from Ascent Technologies. Rotenone was a kind gift from Dr. Timo Myöhänen (Faculty of Pharmacy, University of Helsinki). CellTiter-Glo Luminescent

Cell Viability Assay (cat. no. G7570) and CytoTox 96 Non-Radioactive Cytotoxicity Assay (cat. no. G1780) kits were purchased from Promega. JC-10 Mitochondrial Potential Assay Kit (cat. no. ab112123) was purchased from Abcam. CM-H₂DCFDA General Oxidative Stress Indicator (cat. no. C6827) was purchased from Life Technologies.

Molecular cloning

The GFP-tagged mitochondrial outer membrane protein-25 (GFP-OMP25) plasmid [28] was a kind gift from Dr. Brendan Battersby (Faculty of Medicine, University of Helsinki). The GFP-OMP25 fragment was cloned into the lentiviral expression vector with synapsin (pLenSyn1) promoter for specific transduction into neurons [29]. The GFP-OMP25 cassette was amplified by PCR (primers used: 5'-CGGGATCCGCCACCATGGTGAGCAA-3' and 5'-CGCGCTCGCGCTATTAGAGCTGCTTTC-3'). Both the PCR fragment and the vector were digested with the restriction enzymes BamHI and XhoI. Following the transformation of XL1 Blue *E. coli* with the new ligated plasmid, colonies were screened by NheI digestion and confirmed by sequencing.

Lentivirus production

Lentiviral particles were produced as described previously [30]. Briefly, HEK-293T cells were cultured in DMEM (supplemented with 10% FBS, 1% Penicillin/Streptomycin and 2 mM L-glutamine) and grown on 10-cm plates to 60–80% confluency. The cells were transfected using Fugene HD (Promega) with 6 μ g of total DNA per plate, including pLenSyn1-GFP-OMP25 (3 μ g) and the viral envelope and packaging plasmids pMD2.G (0.75 μ g) and pPAX2 (2.25 μ g), respectively. The supernatant was collected 45 hours post-transfection and precleared by centrifugation at 900 rpm 3 times for 5 minutes. Viral particles were collected by centrifugation at 50,000 \times g for 2 hours, resuspended in plain DMEM and stored at –80°C prior to use.

Preparation of primary neurons and lentiviral transduction

Cerebellar granule neurons (CGN) and hippocampal neurons (HCN) were prepared as described previously [30]. Briefly, CGN were prepared from P6–P8 NMRI mice and HCN from E18 Wistar rat embryos. Brain tissues were dissected and cleaned of membranes in cold PBS supplemented with 0.25% glucose, 0.3% bovine serum albumin (BSA), and 0.038% MgSO₄. Tissues were trypsinized for 15 minutes in a +37°C water bath. CGN were plated on poly-L-lysine (Sigma) coated cell culture plates at a density of 0.325–0.5 million cells per ml and HCN at a density of 0.15–0.2 million cells per ml. HCN were grown in Neurobasal (Gibco) supplemented with 2% B27, 2 mM L-glutamine, and 1% Penicillin/Streptomycin. CGN culture medium included additional 0.5% FBS and 25 mM potassium chloride, required for sustaining CGN cultures *in vitro*. Neurons were cultured for 6–7 days before the start of treatments. CGN were transduced at 4 DIV and cultured for 72–96 hours prior to the start of treatments.

Treatments

BBR was prepared freshly before each set of experiments by dissolving in DMSO as a 20 mM stock solution. Culture concentrations (0.01–10 μ M) were made by serial dilutions into plain Neurobasal medium with total DMSO content remaining below 0.1%. Neurons were treated with BBR for 0.5–24 hours, as indicated in the data. For cotreatment experiments, neurons were pretreated with z-VAD-FMK (100 μ M), FK-506 (1 μ M), CsA (1 μ M), memantine (10 μ M), and MK-801 (1 μ M) for

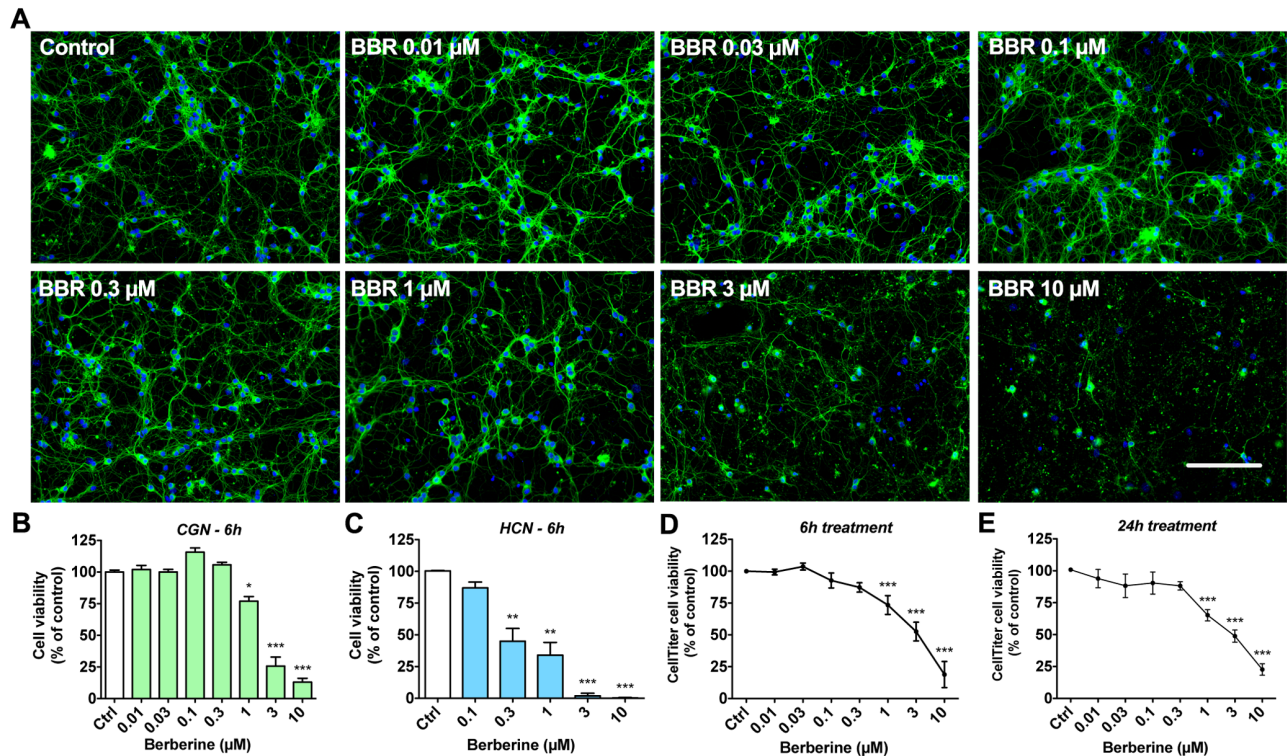


Figure 1. Dose-dependent neurotoxicity of berberine in primary neurons. Primary neurons (cerebellar granule neurons [CGN; DIV7] and hippocampal neurons [HCN; DIV7]) treated with BBR for 6 hours at concentrations between 0.01 and 10 μM indicate a clear dose-dependent loss of neuronal cell viability with IC_{50} of roughly 3 μM . (A) CGN were stained for visualization of neurite (β -tubulin III, TUJ1) and nuclear (Hoechst 33342) morphology at 20X magnification. (B) Neuronal cell viability assessed by visual scoring of CGN nuclear morphology after 6-hour treatment with BBR. (C) Neuronal cell viability assessed by visual scoring of HCN nuclei morphology after 6-hour treatment with BBR. (D) Neuronal viability of CGN, as assessed by CellTiter-Glo assay measuring cellular ATP content, for 6-hour treatments with the indicated BBR concentrations. (E) Neuronal viability of CGN, as assessed by CellTiter-Glo assay for 24-hour treatments with the indicated concentrations. For A, green is β -tubulin III, blue is Hoechst; the scale bar represents 100 μm . For panels B, D, E, $n=5$. For C, $n=3$. For B–E, * = $p<0.05$, ** = $p<0.01$, *** = $p<0.001$. doi:10.1371/journal.pone.0107129.g001

1 hour before the addition of BBR for additional 6 hours. For BBR preconditioning experiments, CGN were pretreated with 30 or 300 nM BBR for 18 hours before the addition of glutamate (20–100 μM) or rotenone (0.1–1 μM) into the culture medium for 6 hours. CGN were deprived by switching to low potassium/serum medium for 6 hours (K5) to induce neuronal apoptosis and caspase-3 activation (Neurobasal supplemented with 0.5% FBS, 1% Penicillin/Streptomycin, 2 mM L-glutamine and 5 mM KCl).

CellTiter-Glo cell viability assay

ATP-based CellTiter cell viability was measured according to the manufacturer's instructions (Promega). Briefly, CGN were plated on 96-well white-walled clear-bottom plates and grown for 7 DIV. After completion of experiments, 100 μl of pre-mixed CellTiter-substrate was added to each well and the plate was shaken for 2 minutes at 200 rpm. The luminescence was then measured (Ex/Em = 560/590 nm) with the Victor³ 1420 Multi-label counter.

Immunofluorescence microscopy

Immunofluorescence (IF) microscopy was performed as previously described [30]. Briefly, cells were grown on poly-L-lysine coated coverslips and fixed for 20 minutes with 4% PFA in PBS before permeabilization for 1 hour in blocking buffer (5% normal serum [goat and donkey], 1% BSA, 0.1% gelatin, 0.1% Triton-

X, 0.05% Tween-20). Primary antibodies used were: β -tubulin III (TUJ1; Covance, mouse and rabbit, 1:1000), TOM-20 (a kind gift from Prof. Anu Wartiovaara [Faculty of Medicine, University of Helsinki]; Santa Cruz, rabbit, 1:1000), and AIF (D39D2; Cell Signaling, rabbit, 1:500). Primary antibodies were incubated overnight at +4°C. The secondary antibodies used were: AlexaFluor-conjugated antibodies (Invitrogen) 488-goat-anti-mouse, 488-donkey-anti-rabbit, 350-goat-anti-mouse, and 568-donkey-anti-rabbit, used at a dilution of 1:2000. Secondary antibodies were incubated for 1 hour at room temperature. Cell nuclei were stained with Hoechst 33342 (Invitrogen, 1:10,000). Images were taken with a Zeiss Imager M1 microscope. ImageJ software was used for cell counting and Adobe Photoshop for the preparation of figures.

Neuronal cell viability

Neuronal cell viability was evaluated by assessing nuclear morphology from immunofluorescence images taken at 20X and 40X magnifications from random fields. The nuclei of TUJ-1-positive cells, identified as neurons, were counted and scored as either normal or condensed as previously described [30]. Neuronal viability was calculated by the following formula: (total neuronal nuclei – condensed neuronal nuclei)/total neuronal nuclei. At least 300 cells per coverslip were counted for each data point.

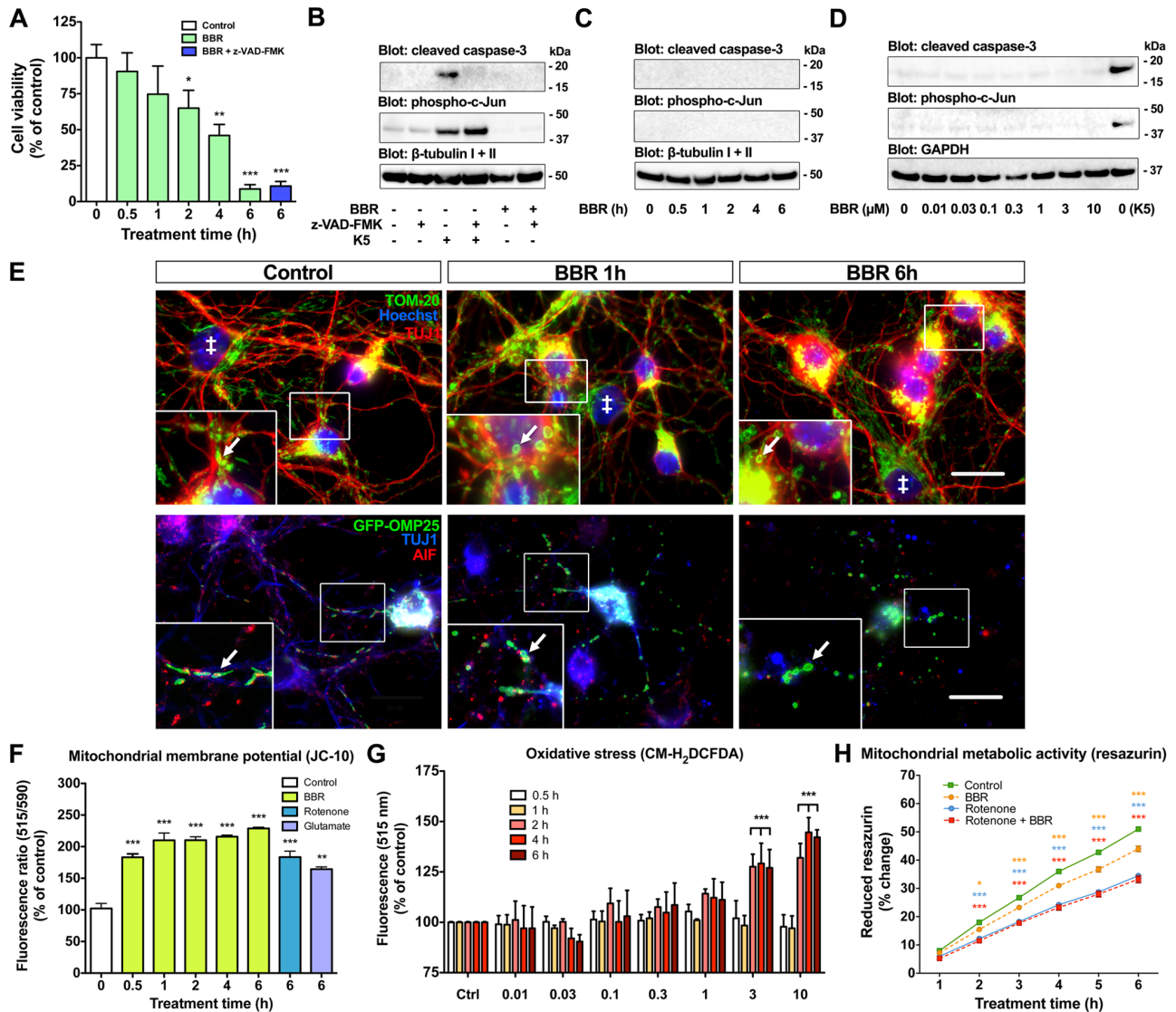


Figure 2. Berberine alters mitochondrial function and morphology, and causes caspase-independent cell death. BBR causes rapid reduction in cell viability independent of caspase-3 activation, and changes in mitochondrial function and morphology. (A) Neuronal cell viability assessed by visual scoring of nuclear morphology reveals the largest drop in viability to take place between 4 and 6 hours. Pan-caspase inhibitor z-VAD-FMK does not affect BBR toxicity after cotreatment for 6 hours. (B) Western blot (WB) of CGN cell lysates shows caspase-3 cleavage and phosphorylation of c-Jun in serum/potassium deprived-neurons (K5) but not in BBR-treated neurons. Cotreatment with z-VAD-FMK prevents caspase-3 cleavage, but c-Jun remains phosphorylated as it functions upstream of caspase-3 in the neuronal apoptosis pathway. (C, D) WB of CGN lysates show that treatment with 10 μ M BBR for 0.5–6 hours (C) or with 0.01–10 μ M BBR for 6 hours (D) does not induce cleavage of caspase-3 or phosphorylation of c-Jun. (E) CGN were stained with TOM-20 (top row) or transduced with GFP-OMP25 lentivirus (bottom row) to visualize all mitochondria and neuronal mitochondria, respectively. Glial cells, marked with ‡, display larger nuclei, and lack of TUJ1-staining (top row). Mitochondria in untreated neurons display an elongated shape, and the proportion of rounded mitochondria (white arrows) is increased by BBR treatment. (F) BBR lowers mitochondrial membrane potential in CGN as evaluated by the increased JC-10 monomer/aggregate ratio (515/590 nm). (G) BBR at 3 and 10 μ M causes a sharp increase in oxidative stress after 2 hours of treatment as assessed by the CM-H₂DCFDA assay. (H) BBR treatment lowers the rate of resazurin reduction, but does not have an additive effect when coupled with maximal complex I inhibition with 10 μ M rotenone. Orange *** indicate significant difference between control and BBR, blue *** indicate significant difference between control and rotenone, and red *** between BBR and BBR + rotenone-treated CGN. For E: (top row) blue is Hoechst, green is TOM-20 and red is β -tubulin III and (bottom row) blue is β -tubulin III, green is GFP-OMP25 and red is AIF; the scale bar represents 20 μ m. For panels A, F, H, n = 4. For panel G, n = 5. For A, F, G and H, * = p<0.05, ** = p<0.01, *** = p<0.001. doi:10.1371/journal.pone.0107129.g002

Western blotting

Western blotting (WB) was performed as previously described [30]. Briefly, cells were lysed in extraction buffer containing 10 mM Tris-HCl, pH 7.6, 2 mM EDTA, 0.15 M NaCl, 1% Triton-X, inhibitor cocktail (1 pill/10 ml; Roche), and 0.25% NP-40 (Sigma). Lysates were cleared by centrifugation at 13,000 \times g for

10 minutes. Samples were denatured with β -mercaptoethanol and heated at 70°C for 10 min before running them in NuPAGE 4–12% Bis-Tris gels (Invitrogen) at 160 V for 60 minutes using the X-Cell SureLock (Invitrogen) gel apparatus. Proteins were transferred to PVDF membranes with a Bio-Rad Trans-Blot Turbo for 25 minutes at 25 V. Membranes were blocked for

1 hour in 5% non-fat milk powder (Valio) diluted in TBST (TBS + 0.1% Tween-20 [Sigma]) before overnight incubation with primary antibodies at +4°C. The primary antibodies used were: cleaved caspase-3 (Asp175; Cell Signaling, rabbit, 1:1000), phospho-c-Jun (Ser65; Cell Signaling, rabbit, 1:1,000), β -tubulin I+II (Sigma, mouse, 1:1000), and GAPDH (6C5; Millipore, mouse, 1:1000). On the next day, membranes were washed 3 times for 10 minutes with TBST and an appropriate secondary antibody was added for 1 hour. Horseradish peroxidase-linked anti-mouse (GE Healthcare, LNA931V) and anti-rabbit (GE Healthcare, LNA934V) secondary antibodies were used at a 1:6000 dilution in TBST. After washing, membranes were soaked for 3 minutes with Pierce ECL reagent (Thermo Scientific, 32106). Protein bands were detected with the LAS-3000 imaging system (Fujifilm). Quantity One software (Bio-Rad) was used for the optical density quantification of Western blots.

CM-H₂DCFDA oxidative stress assay

CM-H₂DCFDA is a probe sensitive to oxidation by reactive oxygen species (ROS) and was used to measure oxidative stress according to the manufacturer's instructions (Life Technologies). Briefly, CGN were cultured on 96-well white-walled clear-bottom plates in phenol-red free Neurobasal media until 7 DIV. Before the start of experiments, all wells were washed once with prewarmed PBS and the cells were loaded with 100 μ l per well of CM-H₂DCFDA (50 μ g diluted in 6 milliliters of PBS) for 30 minutes at 37°C. Fresh phenol-red free Neurobasal media and BBR treatments (BBR 0.01–10 μ M) were added to the wells after loading. The fluorescence was measured (Ex/Em = 485/515 nm) with the Victor³ 1420 Multilabel counter after 0.5, 1, 2, 4 and 6 hours post-treatment.

JC-10 mitochondrial membrane potential assay

Mitochondrial membrane potential was measured according to the manufacturer's instructions (Abcam). Briefly, CGN were cultured on 96-well white-walled clear-bottom plates in phenol-red free Neurobasal until 7 DIV. Thirty minutes before the end of the treatment, 50 μ l of JC-10 dye-loading solution was added to each well and incubated for 30 minutes before measuring fluorescence intensities (Ex/Em = 485/515 nm and Ex/Em = 540/590 nm). The change of mitochondrial membrane potential was measured as the ratio between aggregate (Em = 515 nm) and monomeric forms (Em = 590 nm) of JC-10. Increasing ratios indicate mitochondrial membrane depolarization.

Mitochondrial metabolic activity assay

The rate of mitochondrial metabolic activity was assessed with the resazurin reduction assay [31]. Briefly, CGN were cultured on 96-well white-walled clear-bottom plates until 7 DIV. Resazurin was added to each well to yield a final concentration of 0.1 mM. BBR and rotenone treatments were added to appropriate wells and the fluorescence intensity of reduced resazurin (Ex/Em = 540/590 nm) was measured hourly with the Victor³ 1420 Multilabel counter for 6 hours, with the maximal reduction (100%) measured after 24 hours from vehicle-treated control wells. Rotenone was used to block complex I activity in order to determine the resazurin reduction rate independent of complex I activity.

LDH cytotoxicity assay

LDH measurements were performed as described in the manufacturer's instructions (Promega). Briefly, 50 μ l of conditioned media from CGN cultures were transferred into 96-well white-walled clear-bottom plates (PerkinElmer) in duplicate and

50 μ l of LDH substrate was added to each well. The plate was incubated for 30 minutes at room temperature in the dark before the addition of 50 μ l stop solution. Freshly prepared culture medium was included as a negative control. After gentle mixing on a plate shaker, absorbance was measured at 490 nm with the Victor³ 1420 Multilabel counter (PerkinElmer).

Statistical analyses

A minimum of three repetitions from at least two different batches of cells were used for each experiment. Microsoft Excel and GraphPad Prism software were used for statistical analyses and generation of graphs. Statistical significance was evaluated with the Student's t-test and ANOVA, with the significance threshold set at $p < 0.05$ (*).

Results

Dose-dependent effects of berberine on the viability of primary neurons

We evaluated the effects of BBR on primary neuron viability by immunofluorescence (IF)-based morphological analysis and the CellTiter-Glo ATP-based cell viability assay. We treated CGN with BBR concentrations ranging from 10 nM to 10 μ M for 6 hours and assessed neuronal viability by visualizing nuclear morphology with Hoechst staining. As shown in Figure 1A, lower (0.3 μ M and under) concentrations of BBR did not significantly affect the gross morphology of the CGN neuritic network, comprising both neuronal dendrites and axons. Treatment with 0.1 μ M BBR caused a modest increase in cell viability determined by nuclear staining (Figure 1B) but not ATP content (Figure 1D). However, concentrations exceeding 1 μ M caused a severe disruption of neuritic and nuclear integrity (Figure 1A). These concentrations reduced cell numbers and increased the percentage of condensed nuclei observed in culture (Figure 1B). In HCN, BBR treatments yielded a similar reduction of viability (Figure 1C), indicating a general neurotoxic property for BBR.

Additionally, we assessed cell viability by measuring the ATP content of the neuronal cultures. Treatments with BBR (0.01–10 μ M) showed a similar decrease in ATP levels after both 6- and 24-hour treatments (Figure 1D, E). Similar to cell viability assessment by nuclear morphology, BBR significantly reduced the neuronal ATP content at concentrations between 1 to 10 μ M, with an IC₅₀ of \approx 3 μ M for both 6- and 24-hour treatment periods. Ten micromolar BBR caused the largest decrease, 81.2 \pm 10.2% in ATP levels (Figure 1D), and a 87.0 \pm 3.0% (Figure 1B) decrease in neuronal cell viability, and a dramatic disruption of neuritic integrity (Figure 1A). Consequently, 10 μ M BBR was used as the most potent toxic dose in further experiments.

Berberine causes functional and morphological alterations of neuronal mitochondria independent of caspase-3 activation

BBR triggers both caspase-dependent and -independent pathways of apoptosis [32–34]. Hence, we assessed the time frame of cell death, and the role of caspases and mitochondria to elucidate the mechanisms of BBR neurotoxicity. In a time interval trial, 10 μ M BBR steadily reduced CGN viability, with the most robust loss of viability taking place between 4 and 6 hours of treatment, dropping from 46.0 \pm 7.6% to 9.0 \pm 2.3% (Figure 2A). Additionally, this loss of viability was insensitive to pan-caspase inhibitor z-VAD-FMK (100 μ M), indicating a caspase-independent pathway (Figure 2A). We verified the efficacy of z-VAD-FMK caspase

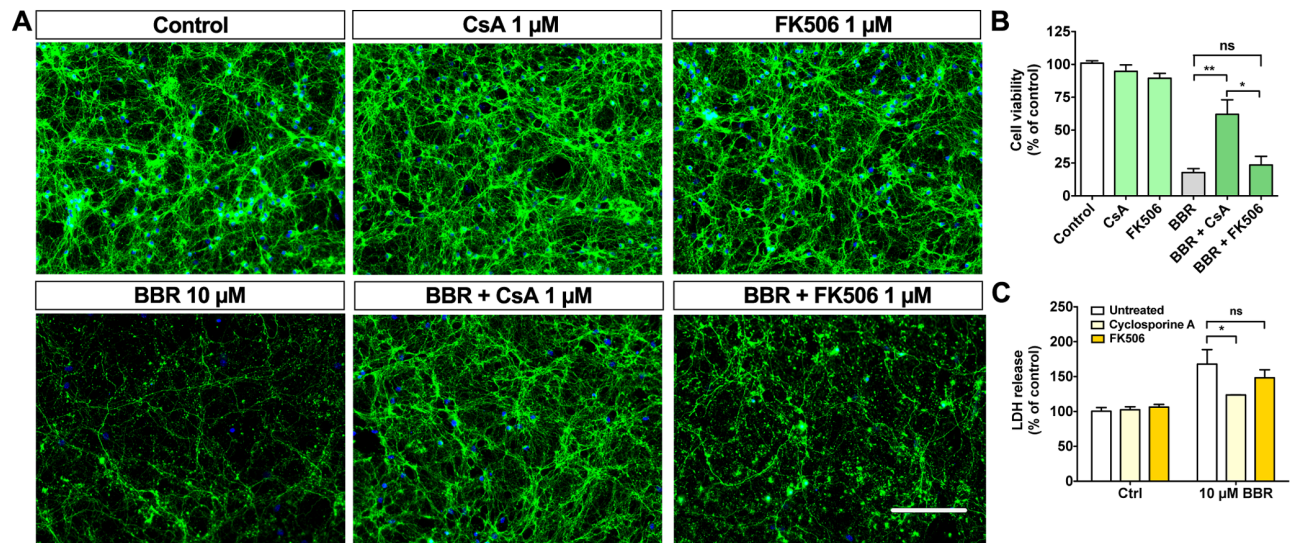


Figure 3. Cyclosporine A partially blocks berberine toxicity. Pretreatment with CsA partially protects CGN against BBR toxicity. (A) Representative images of CGN pretreated 1 hour with and without 1 μM CsA or FK506 before the addition of 10 μM BBR. (B) Quantification of CGN cell viabilities shown in A. (C) LDH release assay from the conditioned media for the described treatments shows partial protection by CsA, but not for FK506. For A, green is β -tubulin III, blue is Hoechst; the scale bar represents 100 μm . For panel B, $n=4$ and for C, $n=3$. For B and C, * = $p<0.05$, ** = $p<0.01$.

doi:10.1371/journal.pone.0107129.g003

inhibition from cell lysates by WB (Figure 2B). The induction of caspase-3 cleavage, the main executioner caspase in neurons, was blocked by z-VAD-FMK during neuronal apoptosis caused by serum/potassium deprivation (K5) leaving the upstream c-Jun phosphorylation unaffected, whereas CGN treated with 10 μM BBR for 6 hours showed no phosphorylation of c-Jun or caspase-3 cleavage (Figure 2B). Additionally, we detected no caspase-3 cleavage or phosphorylation of c-Jun in CGN treated with 10 μM BBR between 0.5–6 hours (Figure 2C) or with BBR concentrations 0.01–10 μM (Figure 2D). These data indicate that BBR-induced neuronal cell death is a rapid caspase-independent process.

Mitochondria are a known target of BBR and a central player in multiple cell death pathways [35]. We assessed the morphological changes of mitochondria by visualizing outer mitochondrial membrane protein TOM-20 by IF-staining (Figure 2E; top row). To better selectively visualize neuronal mitochondria, we transduced CGN with synapsin-promoter driven expression of GFP-OMP25 [28,29] coupled with IF-staining (Figure 2E; bottom row). BBR treatment induced mitochondrial morphological changes in TUJ1-positive cells resembling swelling already after one hour (white arrows in Figure 2E). In contrast to control cells, BBR increased the proportion of spherical mitochondria (Figure 2E). These morphological changes indicate that BBR induces mitochondrial swelling, known to associate with the opening of the mitochondrial permeability transition pore (PTP), a drop in the mitochondrial membrane potential and loss of mitochondrial Ca^{2+} retention [22,35].

In order to elucidate a possible mechanism for mitochondrial swelling, we further explored the effects of BBR on the mitochondrial membrane potential and oxidative stress. Mitochondrial membrane potential was assessed by fluorescent JC-10 that selectively enters the mitochondria forming reversible aggregates as the mitochondrial membrane becomes more polarized, shifting the emitted light from 515 nm (monomeric form) to 590 nm (aggregate form). The mitochondrial membrane potential in CGN treated with 10 μM BBR dropped already after

30 minutes as indicated by the increase in monomer/aggregate ratio (Figure 2F). Treatments with 10 μM rotenone and 100 μM glutamate show a similar loss of membrane potential after 6 hours (Figure 2F). In contrast, oxidative stress increased in neurons treated with 3 and 10 μM BBR only after 2 hours (Figure 2G), coinciding with a decrease in viability seen in Figure 2A. Lastly, the effect of BBR on mitochondrial metabolism was assessed by resazurin reduction assay. BBR lowered the rate of resazurin reduction during 2 to 6 hours of treatment (yellow *) from $18.0\pm 0.4\%$ to $15.5\pm 0.5\%$ at 2 hours, and from $51.0\pm 0.6\%$ to $44.0\pm 1.0\%$ at 6 hours (Figure 2H). Full inhibition of mitochondrial complex I with 10 μM rotenone significantly reduced the rate of resazurin reduction but was not further lowered by BBR treatment (Figure 2H) suggesting that BBR and rotenone do not have an additive effect on mitochondrial metabolism. These data indicate that mitochondrial membrane depolarization and mitochondrial swelling precede an increase in oxidative stress and loss of cell viability in neurons exposed to BBR.

Cyclosporine A partially protects neurons from BBR toxicity

Cyclosporine A (CsA) is a potent PTP inhibitor used as an immunosuppressant and to prevent cardiac hypertrophy following ischemic or reperfusion injuries. Moreover, CsA has been proposed to interact with herbal supplements, such as berberine [36,37]. We used CsA to elucidate whether BBR-induced neurotoxicity is dependent on the PTP formation. Our data indicate that CsA can partially protect neurons from BBR-induced neurotoxicity (Figure 3A), as cell viability improved from $13.3\pm 2.8\%$ to $63.5\pm 11.4\%$ in the presence of 1 μM CsA as assessed by nuclear morphology (Figure 3B). The release of LDH was also reduced from $168\pm 20.7\%$ to $124\pm 0.3\%$ (Figure 3C). Since CsA also inhibits calcineurin activity, we also assessed the effect of FK506, a specific calcineurin inhibitor that has no effect on PTP, on the viability of BBR-treated CGN. FK506 failed to protect CGN from BBR neurotoxicity (Figure 3B, C). These data further highlight the importance of mitochondria in BBR-

mediated toxicity and suggest that PTP formation is involved in mediating the neurotoxic effects of BBR.

NMDA receptor antagonists memantine and MK-801 prevent berberine toxicity

Excitotoxic neuronal cell death is often accompanied by formation of the mitochondrial PTP and release of pro-apoptotic factors from mitochondria to cytosol [38,39]. NMDA receptors and mitochondria are functionally coupled in many types of neuronal cell death [40]. The time course of BBR-induced cell death is faster than in programmed apoptosis and resembles mixed necroptosis occurring during excitotoxic injury [30,41,42]. Glutamate excitotoxicity in neurons is characterized by mitochondrial defects, increased intracellular Ca^{2+} and activation of caspase-independent cell death pathways, and can be prevented by blocking NMDA receptors [43,44]. To elucidate whether BBR toxicity is dependent on NMDA receptor function, we pretreated CGN with NMDA receptor antagonists MK-801 or memantine for 1 hour before the addition of 10 μ M BBR for 6 hours. Both NMDA receptor antagonists preserved neuritic network morphology and completely blocked BBR-induced cell death (Figure 4A, B). Similarly to CGN cultures, NMDA receptor antagonists also prevented BBR toxicity in HCN (Figure 4A, C). These pharmacological data suggest that NMDA receptors are centrally involved in BBR neurotoxicity.

Berberine pretreatment sensitizes neurons to glutamate excitotoxicity

Although our results suggest that BBR is neurotoxic at low micromolar concentrations, previous research indicates that low nanomolar BBR pretreatment can elicit neuroprotection in neuronal-type cells against hypoxic and ischemic insults [16]. As glutamate excitotoxicity is the primary cause of neuronal cell death in ischemic stroke, we tested whether nanomolar BBR can either sensitize neurons to or protect them from glutamate excitotoxicity. Previous research has determined a subtoxic range of glutamate exposure in CGN between 20–50 μ M, whereas 100 μ M glutamate produces prominent excitotoxicity within 6 hours [45,46]. We pretreated CGN for 18 hours with 30 or 300 nM BBR (well-tolerated concentrations; Figure 1) before the addition of 20, 50, or 100 μ M glutamate for an additional 6 hours. When pretreated with 300 nM BBR, CGN became more susceptible to glutamate excitotoxicity, as evidenced by neuritic degeneration (Figure 5A), nuclear condensation (Figure 5B), and LDH release (Figure 5C). Although displaying a similar trend of sensitization as 300 nM BBR, pretreatment with 30 nM BBR did not significantly either increase or reduce neuronal viability. These data suggest that subtoxic nanomolar BBR concentrations are sufficient to sensitize neurons to glutamate excitotoxicity [47].

Nanomolar BBR sensitizes neurons to rotenone injury

The interlinked roles of NMDA receptors and mitochondria are central to excitotoxic injuries resulting from glutamate exposure

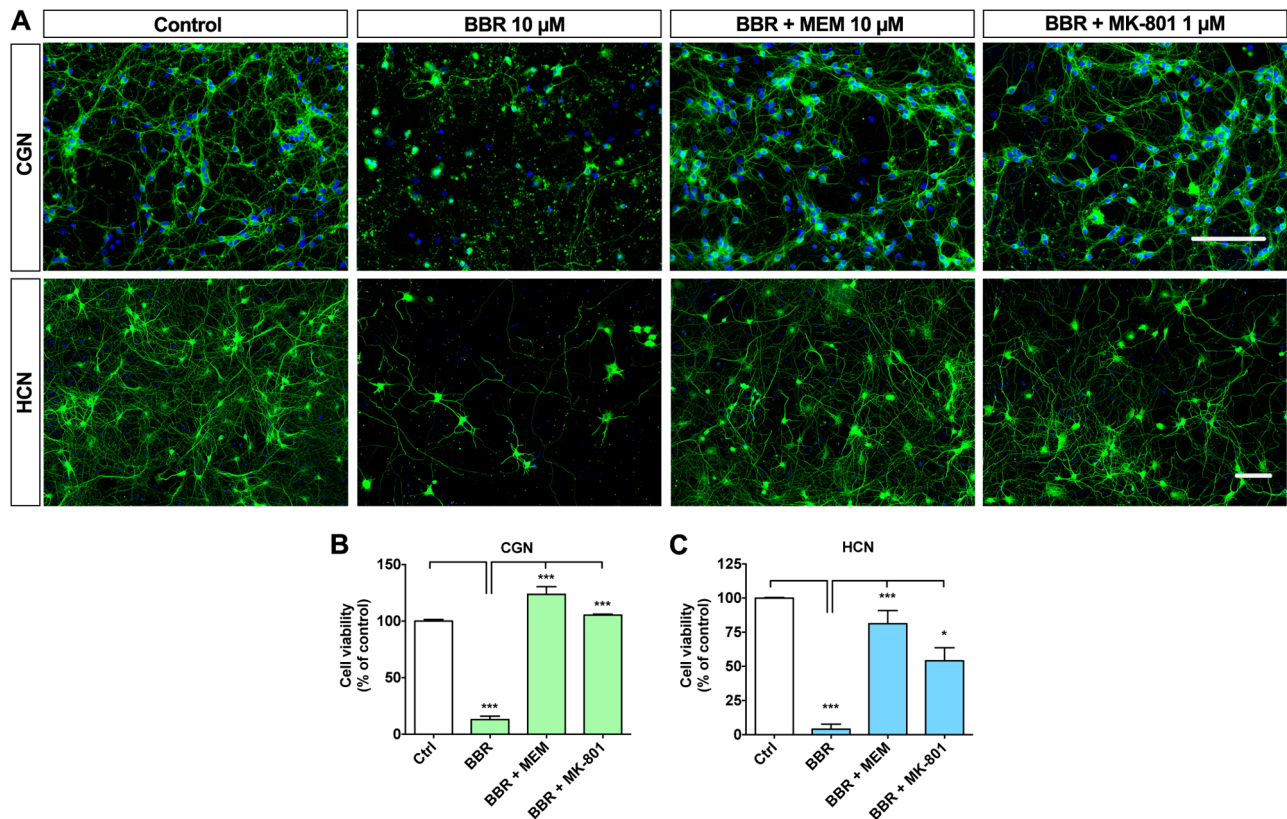


Figure 4. NMDAR antagonists memantine and MK-801 block BBR-induced cell death. NMDA receptor antagonists memantine and MK-801 block toxicity caused by 10 μ M BBR in CGN and HCN cultures. (A) Representative IF images of CGN (upper row) and HCN (lower row) pretreated with memantine and MK-801 before the addition of 10 μ M BBR for 6 hours. (B) Quantification of CGN viabilities shown in A. (C) Quantification of neuronal cell viability of IF images of HCN. For A, green is β -tubulin III, blue is Hoechst; the scale bars represent 100 μ m. For panels B and C, n = 3. For B and C, * = $p < 0.05$, *** = $p < 0.001$. doi:10.1371/journal.pone.0107129.g004

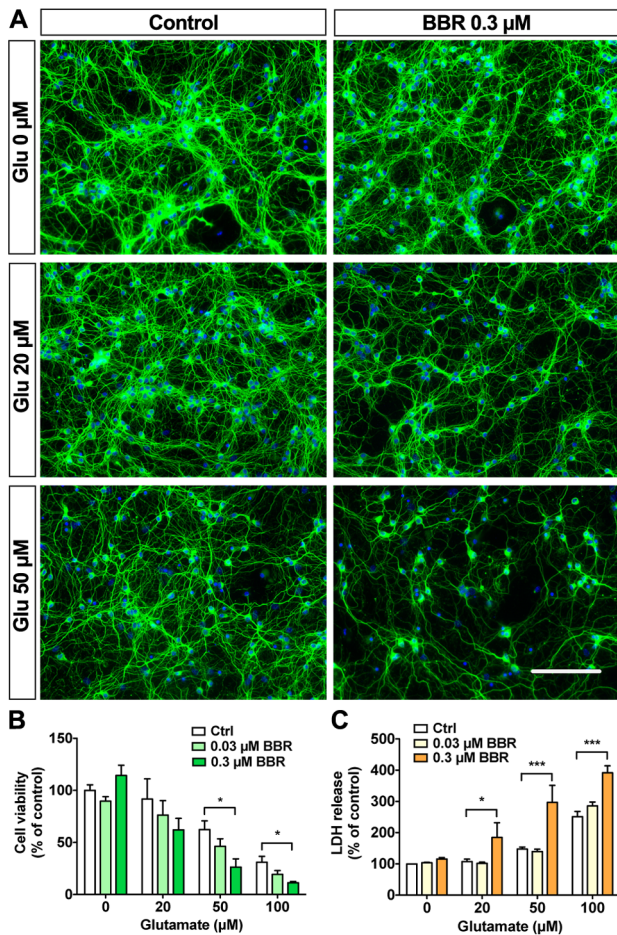


Figure 5. Berberine sensitizes neurons to glutamate toxicity. Pretreating CGN 18 hours with 300 nM BBR exacerbates glutamate excitotoxicity. (A) Representative IF images for CGN pretreated with 300 nM BBR for 18 hours before the addition of 20 or 50 μM glutamate for 6 hours. (B) Quantification of CGN cell viabilities shown in A. (C) LDH release assay from the conditioned media for the described treatments shows exacerbation of toxicity by 300 nM BBR with glutamate co-treatments. For A, green is β-tubulin III, blue is Hoechst; the scale bar represents 100 μm. For panels B, n=3 and panel C, n=4. For B and C, * = p<0.05, *** = p<0.001. doi:10.1371/journal.pone.0107129.g005

and perturbations in the respiratory chain [40,41,48]. Mitochondrial complex I is a common target of pesticides, including rotenone, which is a potent mitochondrial complex I inhibitor with an IC₅₀ of ≈2 μM [49,50]. Moreover, BBR is suggested to directly interfere with mitochondrial complex I [11]. Rotenone is particularly toxic to dopaminergic neurons and is commonly used in Parkinson's disease models [51]. In CGN, rotenone causes acute toxicity within an hour at 5 μM [52] and 10–20 nM levels severely restrict the oxidative respiration rate [40]. BBR has properties similar to these known mitochondria-targeting toxins, as discussed by Shin et al. [19]. We investigated the effects of BBR pretreatment on rotenone toxicity. Our data indicated that 1 μM rotenone caused rapid toxicity within 6 hours, whereas 0.1 μM rotenone did not significantly affect CGN gross morphology and cell viability following a 6-hour treatment (Figure 6A). However, 30 nM BBR pretreatment for 18 hours dramatically sensitized CGN to rotenone treatment, decreasing cell viability from 88.3±4.3% down to 16.0±7.2% in the presence of 0.1 μM rotenone as assessed by nuclear morphology (Figure 6B) and LDH

release assay (Figure 6C). Interestingly, the neuronal network remained relatively intact following rotenone treatment, suggesting a more prominent effect on the neuronal soma than the neuritic network. These data indicate the central role of NMDA receptors and mitochondria in BBR neurotoxicity and that subtoxic levels of BBR can sensitize neurons to excitotoxicity and mitochondrial toxins [53].

Discussion

In this study, we explored the concentration-dependent effects of BBR, a widely used nutraceutical, on the viability of cultured primary neurons. In contrast to the general view of BBR as a neuroprotective nutraceutical, we report that BBR causes neurotoxic effects on cultured cerebellar granule neurons (CGN) and hippocampal neurons (HCN). Low micromolar BBR concentrations induced rapid caspase-independent cell death, which was associated with functional and morphological alterations of mitochondria. Neurotoxicity of BBR was completely blocked by the NMDA receptor antagonists memantine and MK-801, with partial protection achieved with the mitochondrial PTP inhibitor

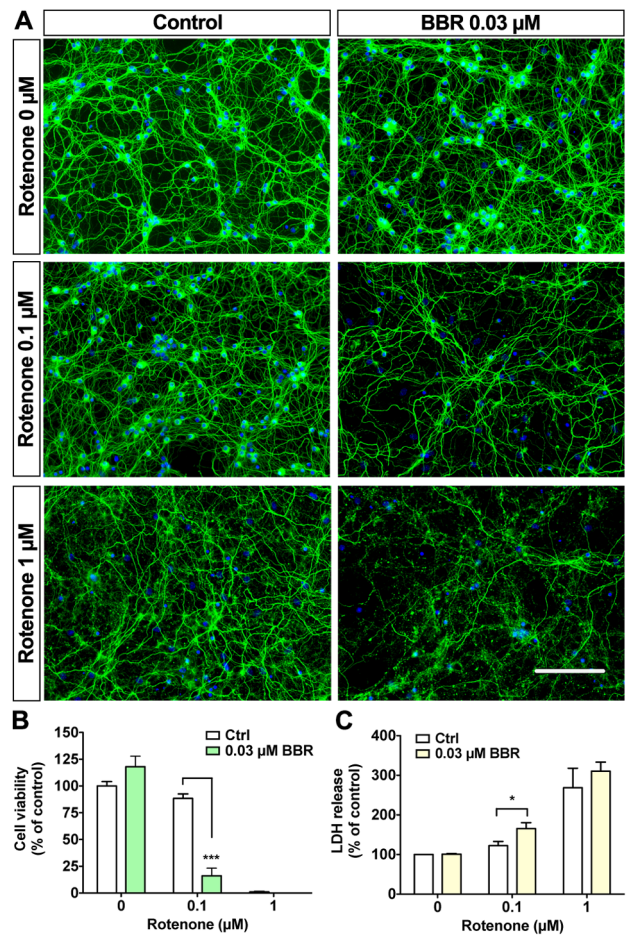


Figure 6. Berberine sensitizes neurons to rotenone-induced injury. Pretreatment with 30 nM BBR is sufficient to sensitize CGN to rotenone toxicity. (A) Representative images of CGN pretreated for 18 hours before the addition of 0.1 or 1 μM rotenone for 6 hours. (B) Quantification of CGN cell viabilities shown in A. (C) LDH release assay shows exacerbation of toxicity by BBR pretreatment. For A, green is β-tubulin III, blue is Hoechst; the scale bar represents 100 μm. For panels B and C, n=3. For B and C, * = p<0.05, *** = p<0.001. doi:10.1371/journal.pone.0107129.g006

cyclosporine A. Additionally, BBR pretreatment sensitized neurons to glutamate and rotenone injury at similar concentrations previously associated with neuroprotection [16]. Our study raises concerns of acute BBR neurotoxicity due to its prominent effects on mitochondria and NMDA receptors, especially when applied at micromolar concentrations close to the levels suggested to be attainable by oral dosing.

BBR is generally well tolerated, as evidenced by its long history of traditional use and several controlled clinical trials in metabolic disorders [5], although use restrictions have been enforced in certain countries, such as Singapore [54,55]. Current literature supports the use of BBR against various indications, ranging from antibiotic and anti-diabetes to anti-cancer and neuroprotection [20]. However, the range of concentrations, treatment times, cell lines, animal models and application methods vary greatly between studies, making direct comparison between published reports difficult. Pharmacological studies on animals and humans suggest that BBR has poor bioavailability. However, while plasma concentrations only reach low nanomolar range, BBR can accumulate in numerous organs, including the brain, reaching low micromolar concentrations [13]. Current attempts to increase the bioavailability of BBR may enhance efficacy when used in metabolic indications, but our study highlights the importance of a thorough safety assessment of BBR in the nervous system. This would be especially important considering the potential long-term use of BBR in the aging population suffering from metabolic diseases, which themselves may increase the risk of ischemic injury and neurodegenerative diseases such as Alzheimer's disease [56].

Our findings support recent evidence that BBR may exacerbate neurotoxicity in dual-hit conditions, as proposed by Myung Koo Lee et al. in Parkinson's disease models [19,57]. Contrary to this view, BBR has been proposed to act as a neuroprotective nutraceutical against various apoptotic insults arising from neurodegenerative conditions such as ischemia and Alzheimer's disease, based on both animal models and several cell lines, including SH-SY5Y, NSC34, and PC12 cells [13,16,18,58–61]. Based on previous literature, however, the effects of BBR on cell viability are highly variable. For example, at low nanomolar concentrations (0.1–10 nM), BBR protects PC12 cells against apoptosis by decreasing caspase activation and ROS generation [27]. However, PC12 cells differ significantly from the primary neurons used in this study. Neurons are generally more sensitive to changes in energy metabolism, excitation and ionic balance in comparison to cell lines [40]. Moreover, PC12 cells lack functional NMDA receptors [62]. These crucial inherent cell physiological differences could explain the robust BBR toxicity observed in primary neurons, leaving many other cell types unaffected at low micromolar concentrations. Whether the protective effects of BBR in PC12 and other cell lines could also be seen with micromolar BBR remains to be seen.

Pro-apoptotic and anti-cancer effects are attributed to high micromolar concentrations of BBR that efficiently inhibit tumor cell proliferation, DNA synthesis, and induce cell cycle arrest [27]. There is evidence for both caspase-dependent and -independent pro-apoptotic roles for BBR [32,33]. We describe BBR-mediated neurotoxicity as a rapid, caspase-independent process. With an IC_{50} of roughly 3 μ M, BBR caused rapid nuclear condensation and fragmentation of neuronal dendrites and axons within 4–6 hours. The radical drop in ATP levels and reduced mitochondrial metabolic activity after micromolar BBR application indicates that BBR causes a severe energy depletion in neurons, resulting in caspase-independent cell death, as ATP would be needed for programmed apoptotic cell death [63]. This

is further supported by the insensitivity of BBR-treated cells to pan-caspase inhibitor z-VAD-FMK and the absence of c-Jun phosphorylation and cleavage of caspase-3, a major executioner caspase.

Mitochondrial targeting is a property of BBR already noted in the 1970s [64,65]. The crucial involvement of mitochondria is evident from the rapid alterations of mitochondrial function and morphology following BBR addition. BBR, and its derivative dihydroberberine, have been shown to specifically target the mitochondrial complex I [11]. Recently, Pereira et al. characterized the effects of BBR on melanoma cell mitochondria as well as isolated mitochondrial fractions [22,35]. They demonstrated that BBR can accumulate in mitochondria causing mitochondrial depolarization and fragmentation, mitochondrial PTP induction, increased oxidative stress, decreased cellular ATP content, and cell cycle arrest [35]. Our results from primary neurons support these findings. While these effects may be desirable for antitumor agents, they may also cause toxicity in neurons, which are sensitive to metabolic disturbances and thus particularly sensitive to mitochondrial dysfunction [40,41,63,66]. Our current results suggest that mitochondria are centrally involved in the toxic effects of BBR in neurons.

In addition to mitochondrial effects, BBR has been reported to modulate ionic currents, particularly via potassium channels [67]. At concentrations similar to the IC_{50} of $\approx 3 \mu$ M for CGN viability, BBR inhibits delayed rectifier currents and HERG channels [15,25,68]. At higher concentrations, BBR also inhibits a variety of potassium currents, including inward and outward rectifier, voltage sensitive, and K^+ channel currents [25,67–69]. The IC_{50} for outward rectifier current is around 10 μ M. Moreover, BBR blocks ATP-sensitive potassium (K_{ATP}) channels with an IC_{50} of 13 μ M, which may cause further depolarization [69]. Interestingly, NMDA receptor composition can be modulated by BBR [70]. We found that the neurotoxic effects of BBR can be completely blocked by inhibition of NMDA receptors, suggesting that modulation of cellular excitability by BBR significantly contributes to its neurotoxic mechanisms.

Our study confirms previous reports on the neurotoxicity of BBR [19,57] and suggests a mechanistic basis to understand how BBR could enhance neurodegenerative processes. These findings raise concerns over the CNS safety profile of BBR, particularly when used in the long-term in the aging population, in patients at risk of silent strokes or ischemic episodes [71], or in people at risk of chronic systemic pesticide exposure [50,72]. Importantly, our results also suggest that memantine, a clinically available NMDA receptor antagonist, may be used to protect neurons against BBR toxicity. Widely available nutraceuticals and dietary supplements have gained considerable interest due to their potential health effects and presumed safety. However, more attention should be paid to both regulatory and research needs in this field.

Acknowledgments

We thank Dr. Roy Siddall for his help on the language revisions, and Dr. Brendan Battersby, Prof. Anu Wartiovaara and Dr. Timo Myöhänen for the provided reagents.

Author Contributions

Conceived and designed the experiments: KK HJH. Performed the experiments: KK CAB. Analyzed the data: KK CAB HJH. Contributed reagents/materials/analysis tools: KK CAB HJH. Contributed to the writing of the manuscript: KK CAB HJH.

References

- Danaei G, Finucane MM, Lu Y, Singh GM, Cowan MJ, et al. (2011) National, regional, and global trends in fasting plasma glucose and diabetes prevalence since 1980: systematic analysis of health examination surveys and epidemiological studies with 370 country-years and 2.7 million participants. *Lancet* 378: 31–40.
- McGill JB (2012) Pharmacotherapy in type 2 diabetes: a functional schema for drug classification. *Curr Diabetes Rev* 8: 257–267.
- Barnes DE, Yaffe K (2011) The projected effect of risk factor reduction on Alzheimer's disease prevalence. *Lancet Neurol* 10: 819–828.
- Imanshahidi M, Hosseinzadeh H (2008) Pharmacological and therapeutic effects of *Berberis vulgaris* and its active constituent, berberine. *Phytother Res* 22: 999–1012.
- Derosa G, Maffioli P, Cicero AF (2012) Berberine on metabolic and cardiovascular risk factors: an analysis from preclinical evidences to clinical trials. *Expert Opin Biol Ther* 12: 1113–1124.
- Benaissa F, Mohseni-Rad H, Rahimi-Moghaddam P, Mahmoudian M (2009) Berberine reduces the hypoxic-ischemic insult in rat pup brain. *Acta Physiol Hung* 96: 213–220.
- Lau CW, Yao XQ, Chen ZY, Ko WH, Huang Y (2001) Cardiovascular actions of berberine. *Cardiovasc Drug Rev* 19: 234–244.
- Jantova S, Cipak L, Cernakova M, Kost'alova D (2003) Effect of berberine on proliferation, cell cycle and apoptosis in HeLa and L1210 cells. *J Pharm Pharmacol* 55: 1143–1149.
- Asai M, Iwata N, Yoshikawa A, Aizaki Y, Ishiura S, et al. (2007) Berberine alters the processing of Alzheimer's amyloid precursor protein to decrease Abeta secretion. *Biochem Biophys Res Commun* 352: 498–502.
- Zhu F, Qian C (2006) Berberine chloride can ameliorate the spatial memory impairment and increase the expression of interleukin-1beta and inducible nitric oxide synthase in the rat model of Alzheimer's disease. *BMC Neurosci* 7: 78.
- Turner N, Li JY, Gosby A, To SW, Cheng Z, et al. (2008) Berberine and its more biologically available derivative, dihydroberberine, inhibit mitochondrial respiratory complex I: a mechanism for the action of berberine to activate AMP-activated protein kinase and improve insulin action. *Diabetes* 57: 1414–1418.
- Yao J, Kong W, Jiang J (2013) Learning from berberine: Treating chronic diseases through multiple targets. *Sci China Life Sci*.
- Durairajan SS, Liu LF, Lu JH, Chen LL, Yuan Q, et al. (2012) Berberine ameliorates beta-amyloid pathology, gliosis, and cognitive impairment in an Alzheimer's disease transgenic mouse model. *Neurobiol Aging* 33: 2903–2919.
- Ji HF, Shen L (2011) Berberine: a potential multipotent natural product to combat Alzheimer's disease. *Molecules* 16: 6732–6740.
- Jung HA, Min BS, Yokozawa T, Lee JH, Kim YS, et al. (2009) Anti-Alzheimer and antioxidant activities of *Coptidis Rhizoma* alkaloids. *Biol Pharm Bull* 32: 1433–1438.
- Zhou XQ, Zeng XN, Kong H, Sun XL (2008) Neuroprotective effects of berberine on stroke models in vitro and in vivo. *Neurosci Lett* 447: 31–36.
- Serafim TL, Oliveira PJ, Sardao VA, Perkins E, Parke D, et al. (2008) Different concentrations of berberine result in distinct cellular localization patterns and cell cycle effects in a melanoma cell line. *Cancer Chemother Pharmacol* 61: 1007–1018.
- Bae J, Lee D, Kim YK, Gil M, Lee JY, et al. (2013) Berberine protects 6-hydroxydopamine-induced human dopaminergic neuronal cell death through the induction of heme oxygenase-1. *Mol Cells* 35: 151–157.
- Shin KS, Choi HS, Zhao TT, Suh KH, Kwon IH, et al. (2013) Neurotoxic effects of berberine on long-term L-DOPA administration in 6-hydroxydopamine-lesioned rat model of Parkinson's disease. *Arch Pharm Res* 36: 759–767.
- Ye M, Fu S, Pi R, He F (2009) Neuropharmacological and pharmacokinetic properties of berberine: a review of recent research. *J Pharm Pharmacol* 61: 831–837.
- Wang X, Wang R, Xing D, Su H, Ma C, et al. (2005) Kinetic difference of berberine between hippocampus and plasma in rat after intravenous administration of *Coptidis rhizoma* extract. *Life Sci* 77: 3058–3067.
- Pereira CV, Machado NG, Oliveira PJ (2008) Mechanisms of berberine (natural yellow 18)-induced mitochondrial dysfunction: interaction with the adenine nucleotide translocator. *Toxicol Sci* 105: 408–417.
- Godugu C, Patel AR, Doddapaneni R, Somagani J, Singh M (2014) Approaches to improve the oral bioavailability and effects of novel anticancer drugs berberine and betulinic Acid. *PLoS One* 9: e89919.
- Ma BL, Ma YM, Shi R, Wang TM, Zhang N, et al. (2010) Identification of the toxic constituents in *Rhizoma Coptidis*. *J Ethnopharmacol* 128: 357–364.
- Rodriguez-Menchaca A, Ferrer-Villada T, Lara J, Fernandez D, Navarro-Polanco RA, et al. (2006) Block of HERG channels by berberine: mechanisms of voltage- and state-dependence probed with site-directed mutant channels. *J Cardiovasc Pharmacol* 47: 21–29.
- Cannillo M, Frea S, Fornengo C, Toso E, Mercurio G, et al. (2013) Berberine behind the thriller of marked symptomatic bradycardia. *World J Cardiol* 5: 261–264.
- Zhang Q, Qian Z, Pan L, Li H, Zhu H (2012) Hypoxia-inducible factor 1 mediates the anti-apoptosis of berberine in neurons during hypoxia/ischemia. *Acta Physiol Hung* 99: 311–323.
- Nemoto Y, De Camilli P (1999) Recruitment of an alternatively spliced form of synaptojanin 2 to mitochondria by the interaction with the PDZ domain of a mitochondrial outer membrane protein. *EMBO J* 18: 2991–3006.
- Vesikansa A, Sakha P, Kuja-Panula J, Molchanova S, Rivera C, et al. (2012) Expression of GluK1c underlies the developmental switch in presynaptic kainate receptor function. *Sci Rep* 2: 310.
- Kysenius K, Muggalla P, Matlik K, Arumae U, Huttunen HJ (2012) PCSK9 regulates neuronal apoptosis by adjusting ApoER2 levels and signaling. *Cell Mol Life Sci* 69: 1903–1916.
- Abu-Amero KK, Bosley TM (2005) Detection of mitochondrial respiratory dysfunction in circulating lymphocytes using resazurin. *Arch Pathol Lab Med* 129: 1295–1298.
- Hwang JM, Kuo HC, Tseng TH, Liu JY, Chu CY (2006) Berberine induces apoptosis through a mitochondria/caspases pathway in human hepatoma cells. *Arch Toxicol* 80: 62–73.
- Wang L, Liu L, Shi Y, Cao H, Chaturvedi R, et al. (2012) Berberine induces caspase-independent cell death in colon tumor cells through activation of apoptosis-inducing factor. *PLoS One* 7: e36418.
- Yuan J, Yankner BA (2000) Apoptosis in the nervous system. *Nature* 407: 802–809.
- Pereira GC, Branco AF, Matos JA, Pereira SL, Parke D, et al. (2007) Mitochondrially targeted effects of berberine [Natural Yellow 18, 5,6-dihydro-9,10-dimethoxybenzo(g)-1,3-benzodioxolo(5,6-a) quinolinium] on K1735-M2 mouse melanoma cells: comparison with direct effects on isolated mitochondrial fractions. *J Pharmacol Exp Ther* 323: 636–649.
- Hausenloy DJ, Boston-Griffiths EA, Yellon DM (2012) Cyclosporin A and cardioprotection: from investigative tool to therapeutic agent. *Br J Pharmacol* 165: 1235–1245.
- Colombo D, Lunardon L, Bellia G (2014) Cyclosporine and Herbal Supplement Interactions. *J Toxicol* 2014: 145325.
- Polster BM, Basanez G, Etxebarria A, Hardwick JM, Nicholls DG (2005) Calpain I induces cleavage and release of apoptosis-inducing factor from isolated mitochondria. *J Biol Chem* 280: 6447–6454.
- Yu SW, Wang H, Dawson TM, Dawson VL (2003) Poly(ADP-ribose) polymerase-1 and apoptosis inducing factor in neurotoxicity. *Neurobiol Dis* 14: 303–317.
- Nicholls DG, Johnson-Cadwell L, Vesce S, Jekabsons M, Yadava N (2007) Bioenergetics of mitochondria in cultured neurons and their role in glutamate excitotoxicity. *J Neurosci Res* 85: 3206–3212.
- Nicholls DG (2008) Oxidative stress and energy crises in neuronal dysfunction. *Ann N Y Acad Sci* 1147: 53–60.
- Fukui M, Choi HJ, Zhu BT (2012) Rapid generation of mitochondrial superoxide induces mitochondrion-dependent but caspase-independent cell death in hippocampal neuronal cells that morphologically resembles necroptosis. *Toxicol Appl Pharmacol* 262: 156–166.
- Volbracht C, van Beek J, Zhu C, Blomgren K, Leist M (2006) Neuroprotective properties of memantine in different in vitro and in vivo models of excitotoxicity. *Eur J Neurosci* 23: 2611–2622.
- Schulz JB, Matthews RT, Henshaw DR, Beal MF (1996) Neuroprotective strategies for treatment of lesions produced by mitochondrial toxins: implications for neurodegenerative diseases. *Neuroscience* 71: 1043–1048.
- Budd SL, Nicholls DG (1996) Mitochondria, calcium regulation, and acute glutamate excitotoxicity in cultured cerebellar granule cells. *J Neurochem* 67: 2282–2291.
- Li CY, Chin TY, Chueh SH (2004) Rat cerebellar granule cells are protected from glutamate-induced excitotoxicity by S-nitrosoglutathione but not glutathione. *Am J Physiol Cell Physiol* 286: C893–904.
- Ward MW, Rego AC, Frenguelli BG, Nicholls DG (2000) Mitochondrial membrane potential and glutamate excitotoxicity in cultured cerebellar granule cells. *J Neurosci* 20: 7208–7219.
- Wang H, Yu SW, Koh DW, Lew J, Coombs C, et al. (2004) Apoptosis-inducing factor substitutes for caspase executioners in NMDA-triggered excitotoxic neuronal death. *J Neurosci* 24: 10963–10973.
- Gomez C, Bandez MJ, Navarro A (2007) Pesticides and impairment of mitochondrial function in relation with the parkinsonian syndrome. *Front Biosci* 12: 1079–1093.
- Betarbet R, Sherer TB, MacKenzie G, Garcia-Osuna M, Panov AV, et al. (2000) Chronic systemic pesticide exposure reproduces features of Parkinson's disease. *Nat Neurosci* 3: 1301–1306.
- Greenamyre JT, MacKenzie G, Peng TI, Stephens SE (1999) Mitochondrial dysfunction in Parkinson's disease. *Biochem Soc Symp* 66: 85–97.
- Isaev NK, Stelmashov EV, Ruscher K, Andreeva NA, Zorov DB (2004) Menadione reduces rotenone-induced cell death in cerebellar granule neurons. *Neuroreport* 15: 2227–2231.
- Johnson-Cadwell LI, Jekabsons MB, Wang A, Polster BM, Nicholls DG (2007) 'Mild Uncoupling' does not decrease mitochondrial superoxide levels in cultured cerebellar granule neurons but decreases spare respiratory capacity and increases toxicity to glutamate and oxidative stress. *J Neurochem* 101: 1619–1631.
- Chan E (1993) Displacement of bilirubin from albumin by berberine. *Biol Neonate* 63: 201–208.

55. Linn YC, Lu J, Lim LC, Sun H, Sun J, et al. (2012) Berberine-induced haemolysis revisited: safety of *Rhizoma coptidis* and *Cortex phellodendri* in chronic haematological diseases. *Phytother Res* 26: 682–686.
56. Carlsson CM (2010) Type 2 diabetes mellitus, dyslipidemia, and Alzheimer's disease. *J Alzheimers Dis* 20: 711–722.
57. Kwon IH, Choi HS, Shin KS, Lee BK, Lee CK, et al. (2010) Effects of berberine on 6-hydroxydopamine-induced neurotoxicity in PC12 cells and a rat model of Parkinson's disease. *Neurosci Lett* 486: 29–33.
58. Lee T, Heo H, Kim Kwon Y (2010) Effect of Berberine on Cell Survival in the Developing Rat Brain Damaged by MK-801. *Exp Neurobiol* 19: 140–145.
59. Cui HS, Matsumoto K, Murakami Y, Hori H, Zhao Q, et al. (2009) Berberine exerts neuroprotective actions against in vitro ischemia-induced neuronal cell damage in organotypic hippocampal slice cultures: involvement of B-cell lymphoma 2 phosphorylation suppression. *Biol Pharm Bull* 32: 79–85.
60. Hsu YY, Chen CS, Wu SN, Jong YJ, Lo YC (2012) Berberine activates Nrf2 nuclear translocation and protects against oxidative damage via a phosphatidylinositol 3-kinase/Akt-dependent mechanism in NSC34 motor neuron-like cells. *Eur J Pharm Sci* 46: 415–425.
61. Hsu YY, Tseng YT, Lo YC (2013) Berberine, a natural antidiabetes drug, attenuates glucose neurotoxicity and promotes Nrf2-related neurite outgrowth. *Toxicol Appl Pharmacol* 272: 787–796.
62. Edwards MA, Loxley RA, Williams AJ, Connor M, Phillips JK (2007) Lack of functional expression of NMDA receptors in PC12 cells. *Neurotoxicology* 28: 876–885.
63. Nicholls DG, Budd SL (2000) Mitochondria and neuronal survival. *Physiol Rev* 80: 315–360.
64. Mikes V, Dadak V (1983) Berberine derivatives as cationic fluorescent probes for the investigation of the energized state of mitochondria. *Biochim Biophys Acta* 723: 231–239.
65. Borodina VM, Zelenin AV (1977) [Fluorescence microscopy demonstration of mitochondria in tissue culture cells using berberine]. *Tsitologiya* 19: 1067–1068.
66. Nunnari J, Suomalainen A (2012) Mitochondria: in sickness and in health. *Cell* 148: 1145–1159.
67. Wu J, Jin GZ (1997) Tetrahydroberberine blocks membrane K⁺ channels underlying its inhibition of intracellular message-mediated outward currents in acutely dissociated CA1 neurons from rat hippocampus. *Brain Res* 775: 214–218.
68. Sanchez-Chapula J (1996) Increase in action potential duration and inhibition of the delayed rectifier outward current I_K by berberine in cat ventricular myocytes. *Br J Pharmacol* 117: 1427–1434.
69. Wang YX, Zheng YM, Zhou XB (1996) Inhibitory effects of berberine on ATP-sensitive K⁺ channels in cardiac myocytes. *Eur J Pharmacol* 316: 307–315.
70. Yoo KY, Hwang IK, Lim BO, Kang TC, Kim DW, et al. (2006) Berberry extract reduces neuronal damage and N-Methyl-D-aspartate receptor 1 immunoreactivity in the gerbil hippocampus after transient forebrain ischemia. *Biol Pharm Bull* 29: 623–628.
71. Goldberg I, Auriel E, Russell D, Korczyn AD (2012) Microembolism, silent brain infarcts and dementia. *J Neurol Sci* 322: 250–253.
72. Tanner CM, Kamel F, Ross GW, Hoppin JA, Goldman SM, et al. (2011) Rotenone, paraquat, and Parkinson's disease. *Environ Health Perspect* 119: 866–872.